Supplementary Data

Fluorescence Resonance Energy Transfer Assays

FRET experiments were conducted using a Horiba Fluorolog 3 spectrofluorimeter equipped with a temperature controller that was thermostated to 20 °C for all FRET experiments. Experiments were carried out in a 1 ml quartz cuvette with a 0.4 cm path-length. Bandpasses for excitation and emission were set to 4 nm and 7 nm, respectively. Buffer conditions for the experiments contained 50 mM HEPES-Na, pH 7.4, 150 mM NaCl, and 1 mM DTT. Experiments were conducted with LSP, HSP1, and NS DNA that was 3´-labeled with TAMRA (acceptor) for the template strand, and 3´-labeled with FAM (donor) for the non-template strand. To measure FRET induced by protein binding to fluorophore labeled DNA, we employed the enhanced sensitization of the acceptor method described in detail by Clegg (1).

This method is described briefly for our particular system. Since spectral overlap exists between FAM and TAMRA, a decrease in the fluorescence emission of FAM at 520 nm and an increase in the fluorescence emission of TAMRA at 580 occur when the end-to-end distance of the DNA and therefore the distance between the fluorophores decrease. DNA bending by TFAM decreases the distance between FAM and TAMRA, and results in an increased FRET effect. The FRET effect (FE) is calculated from the following equation:

$$FE = I_{490}/I_{560} \qquad (1)$$

where I_{490} is the fluorescence emission of the extracted TAMRA signal at 580 nm when excited at 490 nm (**Fig. S3A**), and I_{560} is the fluorescence emission of TAMRA at 580 nm when excited at 560 nm where FAM does not absorb (**Fig. S3B**). The extracted TAMRA signal is obtained by fitting the spectrum of the appropriate 3´-FAM only labeled DNA excited at 490 nm to the donor region of the of the dual labeled DNA spectra exited at 490 nm and subtracting the

fluorescence intensity of the 3´-FAM only labeled DNA from the dual labeled DNA (**Fig. S3C-E**). A plot of the raw FE versus [TFAM] is shown in **Fig. S3F.** The plot of the normalized FE versus the concentration of protein titrated (**Fig. 5A and B**) was used to calculate the dissociation constant (K_{Dapp}) of TFAM and TFAM 1-179 to LSP, HSP1, and NS DNA using a cooperative binding model (Hill) $Y=(B_{max}*x^n)/(K_d^n+x^n)$, where B_{max} is the maximum intensity of FRET effect, K_d is the dissociation constant in mol/L, and n is a measurement of cooperativity, and the ligand depletion binding model $Y=((B_{max})*(((DNA+x+K_d)-sqrt(((DNA+x+K_d)^2)-(4*x*DNA)))/(2*DNA)))$. When the data in **Fig. 5B** were fitted with a ligand depletion model, we measured similar values for LSP, HSP1, and NS DNA of 9.8 ± 1.3 nM, 6.1 ± 1.3 nM, and 6.7 ± 2.3 nM respectively. The error associated with these values is higher than for values obtained using a cooperative binding model; therefore, we reported values obtained from the cooperative fit (**Table 1**). Note that TFAM binding did not directly quench either fluorophore (**Fig. S3G,H**).

Measured $K_{Dapparent}$ values obtained from FRET experiments can readily be converted to ΔG values using the following equation:

$$\Delta G = -RT \ln K \qquad (2)$$

where R is the gas constant of 8.314 J/mol•K, T is the temperature measured in Kelvin, and K is the association constant with units of 1/M and is equal to $1/K_{Dapparent}$.

FE can be used to measure the distance between the FAM donor and the TAMRA acceptor since the distance between donor and acceptor varies as a function of the sixth power of the efficiency of FRET (E) (1,2), as follows:

$$FE = E[\varepsilon FAM_{490}/\varepsilon TAMRA_{560}] + \varepsilon TAMRA_{490}/\varepsilon TAMRA_{560} \qquad (3)$$

The values of $\varepsilon FAM_{490}/\varepsilon TAMRA_{560}$ and $\varepsilon TAMRA_{490}/\varepsilon TAMRA_{560}$ are constants and were calculated to be 0.511 and 0.112 for LSP DNA, 0.509 and 0.109 for HSP1 DNA, and 0.501 and

0.109 for NS DNA, respectively, as previously described (1,3). One can then solve for E and the distance between the FRET donor and acceptor (D_{da}) can be calculated from the following equation:

$$D_{da} = ((1/E)-1)^{1/6})D_r \quad (4)$$

where D_r is the Förster radius for the two fluorophores used in this experiment. D_r values of 58.39 Å, 58.94 Å, and 58.72 Å were calculated NS, HSP1, and LSP DNA, respectively, as previously described (1). Slight differences in D_r values for the different DNA fragments is not surprising since the 3´-regions of the DNA where the fluorophores are tethered are different for all three DNA fragments used in this study. Thus, D_{da} describes end-to-end distance of the DNA and change (Δ) in D_{da} provides information on the degree to which the DNA is bent. In the absence of protein, the calculated D_{da} values for LSP, HSP1 and NS DNA were, 82.3 ± 0.8 Å, 78.1 ± 1.4 Å, 77.1 ± 1.0 Å, respectively. If one assumes that the upon protein binding, the DNA is bent at the middle of the DNA sequence, an estimate of the bend angle can be made using the following equation:

$$\text{Bend angle} = 2\cos^{-1}(D_{da}/^{\circ}D_{da}) \quad (5)$$

where D_{da} is the end-to-end distance in the presence of a given concentration of protein, and $^{\circ}D_{da}$ is the end to end distance in the absence of protein.

Supplementary Figures

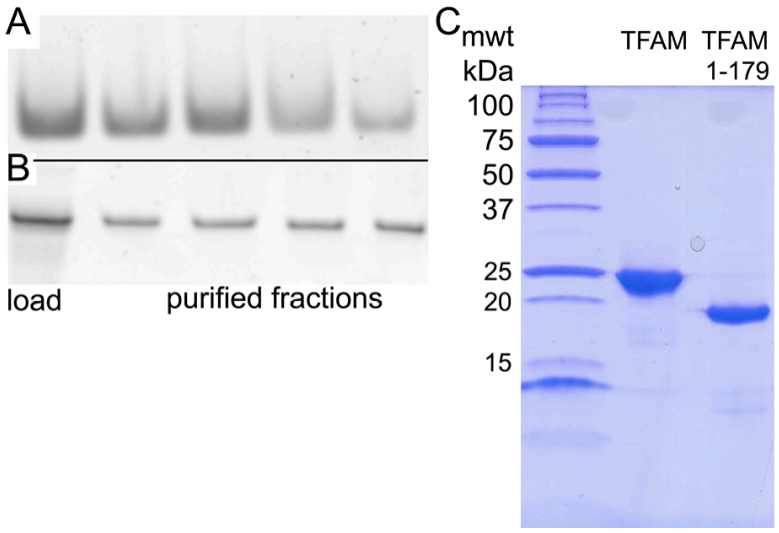

Figure S1. Purified DNA and Proteins.

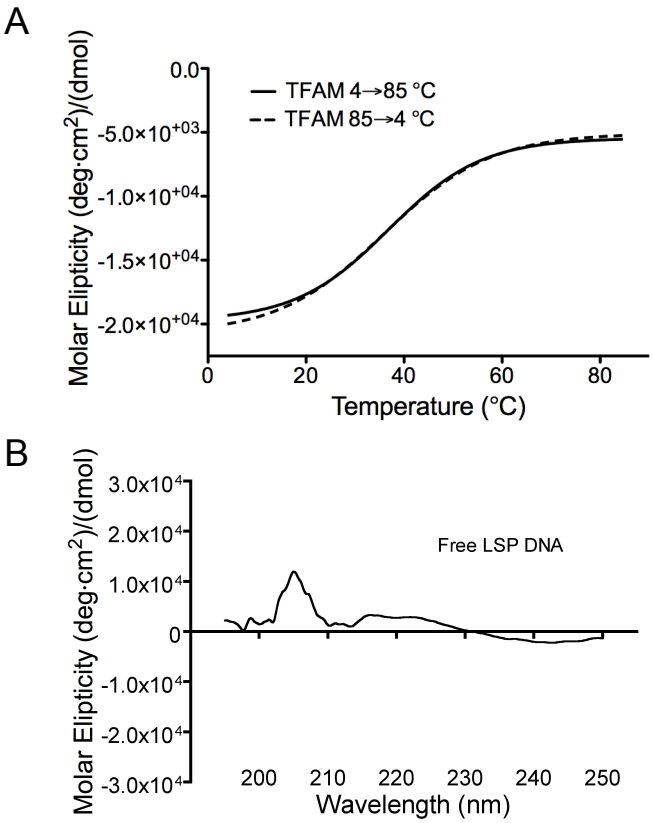

Figure S2A. Thermal denaturation of TFAM shown in Figure 2 is reversible and the DNA contribution to the CD signal at 222 nm is minimal.

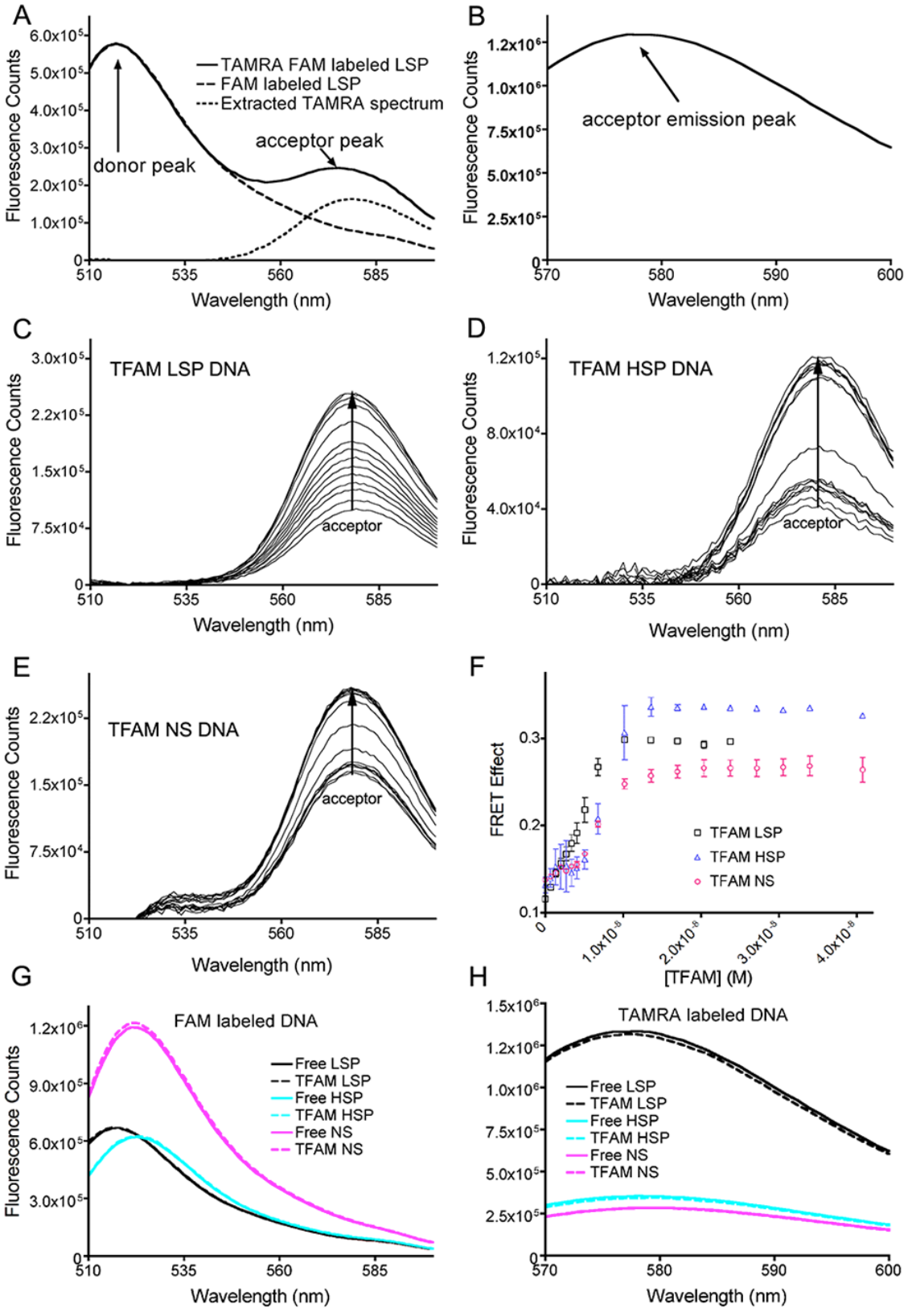

Figure S3. Analysis of the FRET data in Figure 4.

Supplementary Figure Legends

Figure S1. Purified DNA and Proteins.

The purified DNA was analyzed by 8 % acrylamide nondenaturing gel (**A**) and 10 % acrylamide 7 M urea denaturing gel (**B**) of 25 bp LSP DNA. The load lane shows the DNA prior to purification on an Xterra C18 column, and the purified fractions were collected from the main peak eluting from the Xterra C18 column. **(C)** A 15 % acrylamide SDS-PAGE gel of purified TFAM (center lane) and TFAM 1-179 (right lane) with molecular weight marker (left lane). The positions of the proteins on the gel correspond to their predicted molecular masses.

Figure S2. Thermal denaturation of TFAM shown in Figure 2 is reversible and the contribution of DNA to the CD signal at 222 nm is minimal.

(**A**) Sigmoidal best fit curves of the reversible thermal denaturation of 10 μM TFAM at 222 nm. The forward melt is depicted by a solid line and the reverse melt by a dotted line. (**B**) CD spectrum of 10 μM LSP DNA. Similar spectra were obtained for HSP and LSP DNA.

Figure S3. Analysis of the FRET data in Figure 4.

(**A**) Fluorescence emission spectra of 3.4 nM 3′-TAMRA 3′-FAM LSP DNA (**–**), and 3′-FAM LSP DNA (---) excited at 490 nm. The spectrum of 3′-FAM LSP DNA was fit to the spectrum of 3′-TAMRA 3′-FAM LSP DNA over the range of 510 to 530 nm where TAMRA does not emit light when excited at 490 nm. The fluorescence intensities of the fitted 3′-FAM LSP DNA emission spectrum were subtracted from the fluorescence intensities of the 3′-TAMRA 3′-FAM LSP DNA over the range of 510 to 600 nm to obtain the extracted TAMRA emission spectrum (⋯)

used for the FRET effect calculations described in Equation 1. (**B**) Fluorescence emission spectrum of 3.4 nM 3´-TAMRA 3´-FAM LSP DNA, and 3´-FAM LSP DNA excited at 560 nm. (**C**) Extracted TAMRA emission spectra of 3.4 nM 3´-TAMRA 3´-FAM LSP DNA, (**D**) HSP1 DNA, and (**E**) NS DNA. Panel **C** was titrated with TFAM over a range of 0 to 23.8 nM TFAM while panels **D** and **E** were titrated with TFAM over a range of 0 to 40.8 nM TFAM. For panels **C, D**, and **E**, the TAMRA acceptor signal increased as the concentration of TFAM increased until saturation was reached. (**F**) Plot of raw FRET effect versus TFAM concentration in the presence of LSP, HSP1, and NS DNA. (**G**) Fluorescence emission spectra of 3.4 nM 3´-FAM DNA in the presence and absence of TFAM. TFAM was present at 23.8 nM in the TFAM-LSP spectrum. TFAM was present at 40.8 nM in the TFAM-HSP and TFAM-NS spectra. (**H**) Fluorescence emission spectra of 3.4 nM 3´-TAMRA DNA in the presence and absence of TFAM. TFAM was present at 23.8 nM in the TFAM-LSP spectrum. TFAM was present at 40.8 nM in the TFAM-HSP and TFAM-NS spectra.

Supplementary References

1. Clegg, R.M. (1992) Fluorescence resonance energy transfer and nucleic acids. *Methods Enzymol*, **211**, 353-388.
2. Stuhmeier, F., Hillisch, A., Clegg, R.M. and Diekman, S. (2000) Fluorescence energy transfer analysis of DNA structures containing several bulges and their interaction with CAP. *J Mol Biol*, **302**, 1081-1100.
3. Dragan, A.I., Klass, J., Read, C., Churchill, M.E.A, Crane-Robinson, C. and Privalov, P.L. (2003) DNA binding of a non-sequence-specific HMG-D protein is entropy driven with a substantial non-electrostatic contribution. *J Mol Biol*, **331**, 795-813.